THE JOURNAL OF PHYSICAL CHEMISTRY A

ARTICLE

pubs.acs.org/JPCA

Measurement of Heterogeneous Reaction Rates: Three Strategies for Controlling Mass Transport and Their Application to Indium-Mediated Allylations

Isabel A. Olson, Wendi A. Bacon, Yessica Y. Baez Sosa, Katherine M. Delaney, Salvador A. Forte, Michael A. Guglielmo, Alexa N. Hill, Katrina H. Kiesow, Rachel E. Langenbacher, Yuhan Xun, Ryan O. Young, and Walter J. Bowyer*

Department of Chemistry, Hobart and William Smith Colleges, Geneva, New York 14456, United States

ABSTRACT: We describe three new strategies for determining heterogeneous reaction rates using photomicroscopy to measure the rate of retreat of metal surfaces: (i) spheres in a stirred solution, (ii) microscopic powder in an unstirred solution, and (iii) spheres on a rotating shaft. The strategies are applied to indium-mediated allylation (IMA), which is a powerful tool for synthetic chemists because of its stereoselectivity, broad applicability, and high yields. The rate-limiting step of IMA, reaction of allyl halides at indium metal surfaces, is shown to be fast, with a minimum value of the heterogeneous rate constant of 1×10^{-2} cm/s, an order of magnitude faster than the previously determined minimum value. The strategies described here can be applied to any reaction in which the surface is retreating or advancing, thereby broadening the applicability of photomicroscopy to measuring heterogeneous reaction kinetics.

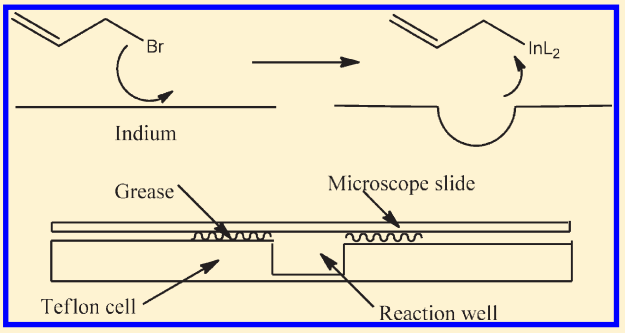

INTRODUCTION

Because of the importance of surface chemistry, there is considerable interest in techniques to measure the rate of heterogeneous reactions.[1] Electrochemical techniques offer a diverse arsenal for measuring electron transfer rates and accompanying chemical reactions at electrode surfaces,[2] but there are relatively few techniques for measuring rates of other heterogeneous reactions.

Three difficulties complicate the measurement of reaction rates at surfaces. First, the initiation time may be variable, so the time at which the reaction begins often is not easily determined. Second, mass transport in a stirred heterogeneous system can be difficult to describe quantitatively. Third, even an apparently uniform surface may not react uniformly, so knowledge of the reactive surface area is difficult. Also, if the reaction alters the surface (for example, by deposition or dissolution), the reactive surface area is even harder to know as it is continuously changing.[3−5]

In situ imaging of surfaces during reaction is a powerful strategy for studying heterogeneous reactions, and various scanning microscopies (e.g., STM, AFM, SECM) have proven especially useful.[1,5,6] For example, scanning electrochemical microscopy (SECM) can detect soluble reactants and products very close to reacting surfaces.[7−9] In situ atomic force microscopy (AFM) has been applied to determine the rate and mechanism of growth and dissolution of crystals.[10,11]

Optical microscopy is a relatively simple alternative strategy for studying rates on reactive surfaces. Early applications combined a sensitive digital camera with chemiluminescence or fluorescence.[12,13] Even more simply, we have been using optical photomicroscopy to quantify reaction rates by measuring the rate of retreat of metal surfaces that are being consumed.[5,14] Fundamental kinetic studies are a powerful tool for exploring mechanisms, and they often assist in the rational selection of conditions for synthesis (e.g., choice of solvent, control of stereochemistry, optimization of yield).[3,15,16]

For example, during the formation of Grignard reagents, organohalides consume solid magnesium (Scheme 1), initially forming hemispherical pits, which grow as the reaction proceeds. Using photomicroscopy to continually determine the surface area and rate of growth of individual reactive sites, we determined heterogeneous rate constants (k_s) from the slope of a plot of the radius of the pits vs time (dr/dt). By making measurements over a range of temperatures, we determined Arrhenius parameters for the reaction, which were consistent with a transition state that is an adsorbed organohalide with a partially broken carbon−halogen bond.[16] Since that time, independent studies supported those kinetic parameters,[17] and density functional theory calculations supported the enthalpy of activation and the proposed transition state.[18] Thus, photomicrographic techniques represent an important addition to the repertoire of tools for measuring heterogeneous reaction rates.

An important heterogeneous reaction similar to the Grignard reaction is indium-mediated allylation (IMA).[19] A wide variety of allyl halides react with solid indium to form an allylindium intermediate (Scheme 2, L = Br or allyl), which can go on to attack a wide variety of electrophiles (second step of Scheme 2).[20]

Received: August 2, 2011
Revised: August 31, 2011
Published: September 01, 2011

Scheme 1

$$\text{R-Br} + \text{Mg}_{(s)} \rightarrow \text{R-Mg-Br}$$

Scheme 2

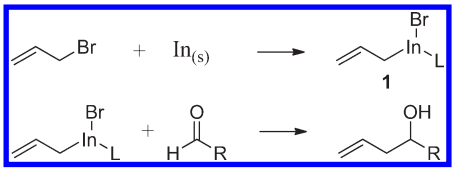

IMAs have received a lot of attention because the reaction proceeds easily and in high yield,[21] is remarkably stereo- and regioselective,[22] and proceeds in aqueous solutions, offering the benefits of Green chemistry.[19−23] Given the importance of IMA, it is remarkable that very few fundamental studies of the reaction have been published.[24,25]

We recently quantified rates for the first, rate-limiting step (the formation of the allylindium intermediate, **1**), by constructing an indium−glass sandwich that constrained the reactivity of the indium to a single face.[26] We then used in situ photomicrography to measure the distance of retreat of the indium surface, x, as a function of time, t. To form the allylindium compound, **1**, two things must happen: the allyl halide must be transported to the indium surface, and then the surface reaction, the breaking and forming of bonds, must occur. Either can be rate limiting. For the geometry of our indium−glass sandwiches, we derived two equations that describe the function of x vs t. If the surface reaction controls the rate, eq 1 describes x vs t as linear. If diffusion controls the rate, eq 2 predicts that x vs t is curved and x vs $t^{1/2}$ is linear. (k_s = heterogeneous rate constant (cm/s); C = concentration of allyl halide (mol/cm^3); n = reaction order; V_m = molar volume of indium (cm^3/mol); D = diffusion coefficient of allyl halide (cm^2/s); b = stoichiometric ratio of In:allyl halide.)[26]

$$x = k_s C^n V_m t \quad (1)$$

$$x = (2DCV_m/b)^{1/2} t^{1/2} \quad (2)$$

For the indium−glass sandwiches, measurements of the retreat of the indium surface during reaction of allyl bromide (ABr) or allyl iodide (AI) were consistent with eq 2 and diffusion control. Measurements over a range of concentrations demonstrated that reactions of both ABr and AI are first order, and we determined diffusion coefficients that were within expectations. Using eq 1 and the steepest portions of the x−t plots, we calculated a minimum value of the heterogeneous rate constant, $k_s \geq 1 \times 10^{-3}$ cm/s, for ABr and AI.[26]

To distinguish mass transport from kinetic control, we use four strategies. First, in some cases, the function of retreat of the surface vs time is different. For example, in the case of indium−glass sandwiches, kinetic control results in a linear x vs t plot compared to a linear x vs $t^{1/2}$ plot under diffusion control. Second, we increase the viscosity of the solvent with minimal change in polarity by adding polyethylene glycol. Third, we compare rates when X = Br vs X = I. The rate of reaction would be expected to increase down the periodic table,[26−28] while the rate of diffusion is expected to decrease slightly.[26] Finally, when solutions are stirred, mass transport will depend on the convection rate, while kinetics will not.[29−32]

In this paper, we apply these strategies in three new geometries, each with a different method of controlling mass transport of allyl halide to the indium surface. Of the three, the slowest mass transport occurs with reaction at an indium sphere (r = 0.5 mm) with stirring by a stir plate and stir bar. The reaction of microscopic spheres (d < 50 μm) with relatively rapid spherical diffusion is slightly faster.[33−36] Most rapid is reaction at indium spheres fixed to a rotating shaft (up to 2000 rpm).

Although our interest is in the formation of organometallic intermediates, in principle these strategies can be applied to any heterogeneous reaction in which the surface is retreating or advancing. Thus, these fundamental studies further develop the application of microscopy to measuring heterogeneous reaction kinetics.

EXPERIMENTAL SECTION

Image Recording and Analysis. For measurement of 1 mm indium spheres, a trinocular Nikon SMZ-U Zoom 1:10 microscope, Diagnostic Instruments monochromatic video camera, Spot version 4.6 software, and an MVI model NCL150 light source were used to obtain and make measurements on the photomicrographs. The calibration of the image system was confirmed each day by photographing a Meleemeter (Edmund Scientific) and measuring the line spacing. For indium powder, a Motic 200 BA 1:100 trinocular compound microscope with 10× and 20× objectives was used for photomicrographs. Photomicrographs were taken at intervals such that four to eight images were obtained over the course of the reaction.

Reagents. Indium powder (325 mesh, 99.99%) and indium spheres (r = 0.5 mm, 99.99%) were obtained from Alfa Aesar. Allyl iodide and bromide were obtained from Acros Organics or Sigma Aldrich and passed down a short column of activated alumina before use. All other reagents and solvents were obtained from Sigma Aldrich or Fisher Scientific and used as received. Reactions were performed at 22 ± 1 °C.

Solvents. One major advantage of allylindium compounds is that they can be formed and reacted in water. However, the reactants are only very slightly soluble in water, and for kinetic measurements, concentrations must be controlled. Thus, we used a mix of water and ethanol (also a common solvent for indium-mediated allylations). The solution was acidified with 0.1 M HCl to keep the metal surface uniformly reactive by preventing precipitation of indium hydroxide.[26]

For allyl iodide (AI) and allyl bromide (ABr) the solvent was 60% ethanol/40% water/0.1 M HCl (abbreviated 60/40/0.1), which dissolved ABr and AI to at least 0.2 M. In some experiments, to increase viscosity with minimal change in solvent polarity, 10% polyethylene glycol (PEG, MM = 1500 g/mol) was added, and the solvent was 50% ethanol/40% water/0.1 M HCl/10% PEG. For measurements with cinnamyl bromide (1-phenyl-3-bromopropene, CinnBr), the solvent was 90% ethanol/10% water/0.1 M HCl (abbreviated 90/10/0.1) in which CinnBr is soluble to at least 0.4 M. Unfortunately, CinnBr is not stable in this medium for long periods, so fresh solutions must be prepared regularly.

Viscosity Measurements. Solvent viscosities were determined using a calibrated Cannon−Frenske viscometer that was equilibrated in a 24.8 °C water bath. The viscosities of the solvents were determined in centistokes by measuring the efflux times in the viscometer in triplicate. These values were then converted to centipoise, cP, using the density of the solvent mix.

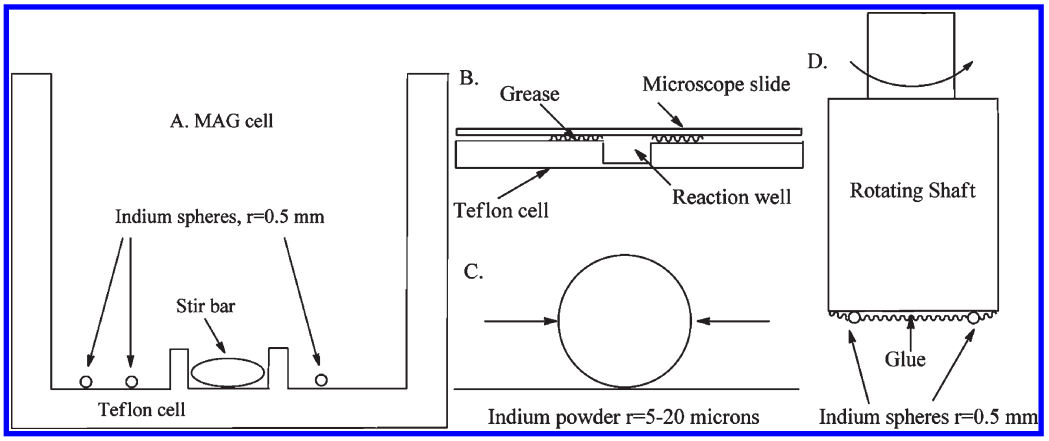

Figure 1. Three geometries for mass transport to indium surfaces. (A) Convection to 1 mm spheres with a stir plate and stir bar. (B) and (C) Diffusion to microscopic spheres. (D) 1 mm spheres on a rotating shaft.

Measuring Reaction Rates. Photomicrography was used to quantify the rate of the reaction. Indium metal is reactive toward allyl halides over the entire surface, and we studied three geometries.

1. Convection to relatively large (r = 0.5 mm) indium spheres in a Teflon cell using a stir bar and stir plate. Indium is very soft, and in our initial efforts the stir bar rapidly deformed the spheres. Thus, a "MAG" cell was designed with a depression to contain the stir bar, surrounded by a moat, where 3−5 indium spheres were introduced (see Figure 1A). Solution (15 mL) (allyl halide dissolved in ethanol/water) was added, a photomicrograph taken, and an airtight lid fixed. Photomicrographs were taken at 0.5−8 h intervals until the spheres were about 50% consumed; fresh solution was introduced after each photograph to ensure the allyl halide concentration did not change significantly during the measurements.
2. Spherical diffusion to very small spheres (325 mesh, r = 5−20 μm). A circular well, 3.6 mm deep and 16 mm wide, was drilled into a Teflon block the length and width of a microscope slide (7.7 cm × 2.5 cm, see Figure 1B and C). The reverse side of the block was then cut until the bottom of the cell was less than 1 mm thick so that either transmitted or reflected illumination could be used. Indium powder (less than 1 mg) was sprinkled on the bottom of the cell; 0.45 mL of the allyl halide solution was introduced; and the well was covered with a microscope slide, with silicon vacuum grease as a seal.
3. Indium spheres on a rotating shaft (see Figure 1D). A Pine Instruments MSR Speed Control and Analytical Rotator (designed for rotating ring-disk electrode measurements) was used to achieve very high mass transport rates with rotations of 100−2000 rpm. A layer of glue slightly less than 0.5 mm thick was spread over the surface of a Teflon cap (r = 8 mm), and four to six indium spheres (r = 0.5 mm) were placed in a circle 2−4 mm from the edge of the cap. On average (N = 62), the spheres protruded 0.6 mm from the glue with a standard deviation of 0.12 mm.

Theory. For allyl halide to react with indium, first the allyl halide must diffuse to the surface, and then bonds must be broken and formed as the reactants surmount the energy of activation barrier. If the energy of activation is sufficiently small, then diffusion will be rate limiting. Stated another way, to measure rapid kinetics, one needs a relatively rapid experiment. For heterogeneous reactions, one way to achieve this is with mass transport rates that are faster than the reaction being studied. Electrochemists have achieved high mass transport rates by a variety of strategies, but these have rarely been applied to other types of heterogeneous reactions.

Here, we derive the equations that describe the radius, r, of a reacting surface as a function of time under kinetic control and under diffusion control.

Kinetic Control. Under kinetic control, the retreat of the surface is independent of the geometry of the indium and independent of the rate of mass transport,[16,26] and the retreat as a function of time is eq 3 (r_o = initial radius). Taking the derivative with respect to time yields eq 4. Thus, a plot of r vs time would be linear under kinetic control.

$$r = r_o - k_s C^n V_m t \tag{3}$$

$$dr/dt = k_s C^n V_m \tag{4}$$

If eq 4 is applied when mass transport is controlling the reaction rate, the calculated k_s is an apparent rate constant, k_{app}, and represents the minimum value of k_s.

Mass Transport Control. In contrast, the equations for mass transport control are not so easily described.[3] In geometry 1 (Figure 1A), convection with a stir bar and stir plate is independent of sphere size. Furthermore, solutions are replaced frequently enough that concentrations do not change significantly. Therefore, the mass transport rate remains constant over the course of the experiment, yielding a straight line for r vs t. Qualitatively, two predictions are apparent if mass transport controls the rate of reaction: (1) increasing the rate of stirring will increase the slope of r vs t and (2) increasing solution viscosity will decrease the slope of r vs t.

In geometry 2 (Figure 1B and C), diffusion to a very small sphere sitting on a nonreactive surface has not been described. However, diffusion to a microhemisphere is well described.[35] Thus, instead of treating the spherical powder particle as whole spheres, they were treated as hemispheres as an approximation. Figure 2 depicts the diffusion layers at 6r for a reactive sphere (gray) and hemisphere (pink) with the same radius. Both the sphere and hemisphere are sitting on the bottom of the welled Teflon cell, and the concentration contours at six radii are shown. The concentration of the allyl halide at 6r and beyond is essentially the same as that in the bulk solution.[33−35]

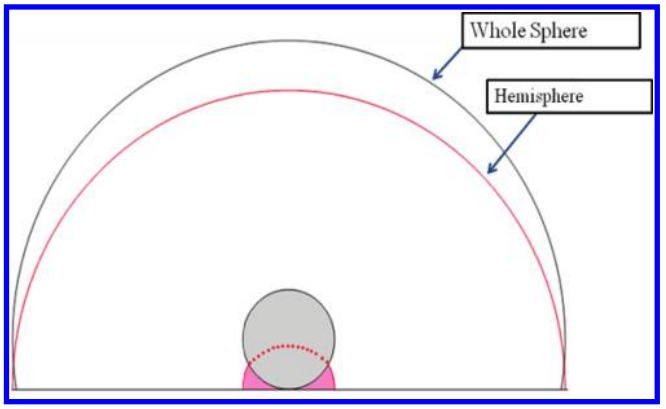

Figure 2. Concentration contours at six radii for a sphere and hemisphere.

Diffusion from an infinite solution to a microhemisphere[35] protruding from the surface is described by

$$\text{Flux} = 2\pi DCr \tag{5}$$

where "Flux" is the rate at which the allyl halide arrives at the surface (mol/s), and r is the radius of the hemisphere (cm). The flux of allyl halide can be converted to the rate of loss of the volume of indium per unit of time

$$dV/dt = \text{Flux}(V_m)/b \tag{6}$$

where b is the stiochiometric ratio of moles of allyl halide reacting per mole of indium, determined to be three allyl halide to two indium, $b = 1.5$.[25,26] The change in volume of a hemisphere as it reacts can be expressed as the rate of change of the radius by

$$dV/dt = 2\pi r^2(dr/dt) = \text{Flux}(V_m)/b \tag{7}$$

Substituting eq 5 into eq 7 and simplifying yields

$$r(dr/dt) = DCV_m/b \tag{8}$$

Integration of eq 8 with respect to time yields

$$\int_r^0 r(dr/dt)dt = \int (DCV_m/b)dt - r^2/2$$

$$= DCV_m t/b + c \tag{9}$$

where $c = -r_o^2/2$, and r_o is the initial radius. Now simplifying eq 9 yields

$$r^2 = r_o^2 - 2DCV_m t/b \tag{10}$$

Thus, the plot of r vs t will not yield a straight line if the reaction is diffusion controlled; rather, the plot will be concave downward. This is qualitatively reasonable as one expects higher flux per surface area as the radius decreases. Inspection of eq 10 predicts that under diffusion control a plot of r^2 vs t yields a straight line with a slope m:

$$m = -2DCV_m/b \tag{11}$$

Equation 11 applies to a hemisphere, but the sphere has twice as much indium as a hemisphere of the same radius. Thus, to calculate an apparent diffusion coefficient, D_{app}, eq 11 was divided by two, allowing calculation of an approximate D_{app} from the slope of r^2 vs t, eq 12. This overcompensates for the difference since there is some diffusion to a sphere that does not occur with a hemisphere, so eq 12 is only an approximation.

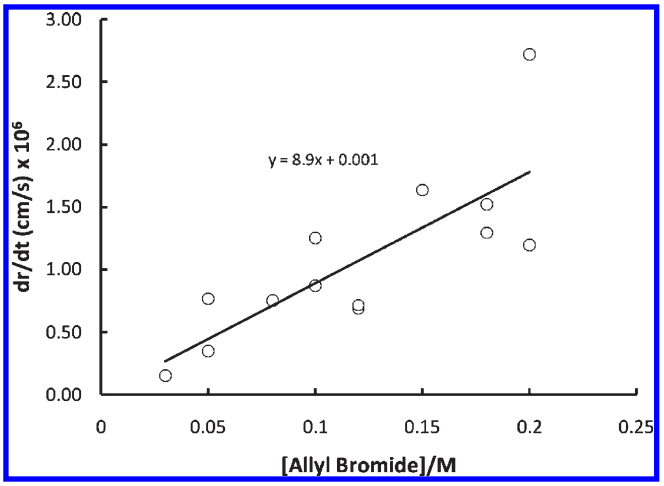

Figure 3. Rate of reaction (dr/dt) vs concentration of allyl bromide/M in MAG cells.

$$m = -D_{app}CV_m/b \tag{12}$$

Making the same argument qualitatively, when the diffusion layer is much larger than the radius of the powder (which on the time scale of these experiments is satisfied by powder that is tens of micrometers in radius), the flux is proportional to the radius of the powder. Therefore, as the radius decreases, the flux will decrease linearly. However, the surface area of the particle decreases with the square of the radius. Thus, under diffusion control, the flux per surface area will increase as the radius decreases, so dr/dt will increase and the plot will be concave downward.

In geometry 3, the spheres are glued to the end of a rotating shaft. Convection-diffusion to a planar rotating disk electrode is well-defined by the Levich equation, eq 13.[2]

$$\text{Flux} = 0.620AD^{2/3}\omega^{1/2}\nu^{-1/6}C \tag{13}$$

where Flux = flux of allyl halide to the surface (mol/s); A = area (cm^2); ω = angular frequency of rotation (s^{-1}); and ν = kinematic viscoscity (cm^2/s). The Levich equation does not apply exactly to the indium hemispheres, which extend above the surface of the rotating plane. However, under mass transport contol, one would expect the flux to be approximately proportional to the square root of the angular frequency, $\omega^{1/2}$. We use our experiments to test the accuracy of the Levich equation in this situation.

RESULTS AND DISCUSSION

MAG Cells: Convection with Stir Plate and Stir Bar. In all of the MAG cell experiments, the radius of the spheres decreased linearly with time as they reacted with allyl halides, consistent with either mass transport or kinetic control. The rate of the reaction (dr/dt) was linearly proportional to the concentration of the allyl halide, again as would be expected for both mass transport or diffusion control. For example, in Figure 3 are the rates (dr/dt) for the reaction of allyl bromide from 0.03 to 0.2 M in 60% ethanol/40% water/0.1 M HCl (60/40/0.1). A linear regression fits the data well and passes very close to the origin. The scatter of the data indicates the reproducibility of convection from one experiment to another, which is limited by the relatively poor control of stir rate with traditional stir plates.

To improve precision for comparability at different stir rates, we constructed matching cells and ran paired experiments with one cell stirring on "high" and the other on "low"; we estimate qualitatively that high stirring is two to three times faster than low. This allowed a test of diffusion vs kinetic control by comparing the effect of stir rate on the rate of the reaction under otherwise similar conditions. In every experiment, the spheres in the high stirring cell reacted more quickly than low stirring, consistent with diffusion control and not kinetic control. For example, in Figure 4 the radii of eight spheres are plotted vs time as they react with 0.06 M cinnamyl bromide. The four spheres in the slow-stirring cell are represented by circles, while those in the fast-stirring cell are squares.

It is possible to convert the rate of reaction, dr/dt, into an apparent rate constant, k_{app}, using eq 4. Under diffusion control, k_{app} represents the minimum value of k_s. These data are collected in Table 1 for the three allyl halides.

The relative standard deviation determined from the replicates in Table 1 was 30%, and a t test demonstrated the differences of k_{app} for high vs low stirring to be significant at >95% for all three compounds. Furthermore, all three compounds, ABr, AI, and CinnBr, react at similar rates. If the rate were kinetically controlled, one would predict that iodides would react much $(10-100\times)$ faster than bromides.[3,27] Inconsistent with expectations for kinetic control, the similarity of the apparent values of k_s again supports that the reaction is mass transport controlled.

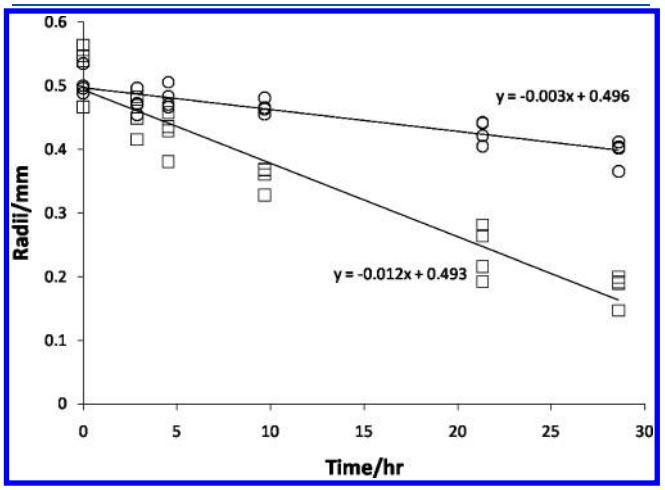

Figure 4. Radii of spheres reacting with 0.06 M cinnamyl bromide in 90/10/0.1 M in MAG cells. Circles: slow stir. Squares: fast stir.

Table 1. Effect of Convection Rate on the Rate of Reaction (Expressed As Apparent Rate Constant, k_{app}) for Three Allyl Halides

allyl halide	k_{app}, high stirring	k_{app}, low stirring	N^a	solvent^b
allyl iodide	4.9×10^{-4} cm/s	2.1×10^{-4} cm/s	9	60/40/0.1
allyl bromide	3.9×10^{-4}	2.2×10^{-4}	5	60/40/0.1
cinnamyl bromide	1.6×10^{-4}	0.73×10^{-4}	7	90/10/0.1

[a] Number of paired experiments. [b] Solvent: ethanol%, water%, HCl/M.

Finally, for ABr, the effect of solvent viscosity was determined by adding 10% PEG. With an approximate doubling of viscosity, the rate of reaction decreased about 2-fold (see Table 2). The difference between with and without PEG is significant at >95%.

Thus, the effect of convection rate, nature of the halide, and viscocity of solvent are all consistent with diffusion control and inconsistent with kinetic control in the MAG cells.

Indium Powder: Mass Transport by Diffusion to Microspheres. It has been well established that diffusion to very small sites can achieve high, steady state mass transport rates.[33−36] Thus, 325 mesh indium powder ($r = 5-20\ \mu$m) was reacted with allyl halides in a cell without stirring. Radii were measured as a function of time with a compound microscope at 100×. As indicated by eqs 4 and 10, if the reaction is kinetically controlled, a plot of r vs t should be linear. Under diffusion control, r vs t is concave downward, while r^2 vs t will be linear.

After measuring radii of almost 100 particles ($N = 96$) as they react in 60/40/0.1 with ABr in concentrations ranging from 0.02 to 0.2 M, plots of r vs t are ambiguous: 74% of the plots appear linear, while 26% appear concave downward. During reaction with AI, $N = 30$ and 57% were better fit with a straight line, while 43% appear concave downward. None of the plots were concave upward. Thus, the data were fit with models for both diffusion and kinetic control.

For those experiments that yielded a plot of r vs t that was concave downward, the data also were plotted as r^2 vs t. In these cases, the resulting plot was linear. The values of D_{app} were calculated for ABr and AI and are collected in Table 3; relative standard deviations suggest that the precision of the reaction rates is 30%. It is satisfying that although the model is not rigorous the values of D_{app} calculated using eq 12 were within 50% of the expected value.[26] Furthermore, these data suggest that diffusion controls the reaction rate.

To test the hypothesis of kinetic control for reaction of ABr and AI with powder, a least-squares fit to those r vs t plots that were linear was used to calculate k_{app} using eq 4. Again, relative standard deviations were 30%. The apparent rate constant is approximately the same for both ABr and AI, supporting that control is by mass transport.

As expected from the relatively rapid rate of diffusion to very small spheres, the apparent rate constants determined with the powder are higher than those determined in a MAG cell (Table 4 compared to Table 1).

Table 3. Apparent Diffusion Coefficient Calculated from Linear Plots of r^2 vs t

allyl halide	D_{app}	N	% of particles
allyl bromide	2.8×10^{-6} cm^2/s	25	26
allyl iodide	2.9×10^{-6}	13	43

Table 2. Values of k_{app} for Determination of the Effect of Viscosity

allyl halide	k_{app}, high stirring	k_{app}, low stirring	N^a	solvent^b	viscosity/cP
allyl bromide	3.9×10^{-4} cm/s	2.2×10^{-4} cm/s	5	60/40/0.1	2.49
allyl bromide/w PEG	2.2×10^{-4} cm/s	1.3×10^{-4} cm/s	5	50/40/0.1/10	4.57

[a] Number of paired experiments. [b] Solvent: ethanol%, water%, HCl/M, PEG %.

dx.doi.org/10.1021/jp207383b |J. Phys. Chem. A 2011, 115, 11001–11007

Table 4. Values of k_{app} Calculated for Those Particles with a Linear r vs t Plot

allyl halide	k_{app}	N	% of particles
allyl bromide	1.9×10^{-3} cm/s	96	74
allyl iodide	2.4×10^{-3}	30	57

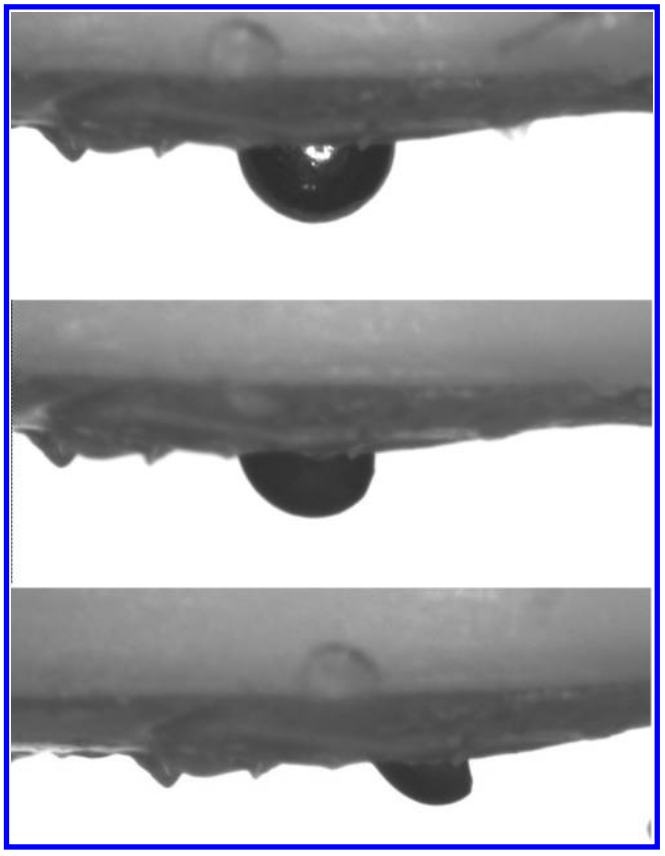

Figure 5. Photographs of an indium sphere during rotation in 0.05 M AI at 1000 rpm. Times: 0 (top), 0.67, and 3.0 h. For scale, the width of the field is 1.9 mm.

Spheres on a Rotating Shaft. As is well demonstrated for rotating electrodes, as the planar surface of the electrode rotates, solution is spun to the sides resulting in convection so that the solution arrives perpendicular to the center of the disk. Indium is very soft, and we found that if an indium sphere was located at the center of the disk the solvent pressure was enough to deform the sphere. In contrast, if the beads were glued 2−4 mm from the edge of the disk, they could withstand rotation rates up to 2000 rpm with no apparent deformation after 24 h.

Figure 5 represents a photomicrograph of an indium bead after 0, 0.67, and 3.0 h of reaction in 0.05 M AI rotating at 1000 rpm. The dimension of the indium from the glue to the top of the bead was measured four to eight times over the course of the reaction and plotted vs time. The rate of retreat is proportional to the allyl halide (AI, ABr, and CinnBr) concentration from 0.01 to 0.2 M, consistent with either mass transport control or kinetic control for a first-order reaction.

The effect of rotation rate on the rate of retreat of the indium surface is illustrated in Figure 6. From 100 to 2000 rpm for 0.1 M ABr in 60/40/0.1, the rate of reaction vs the square root of

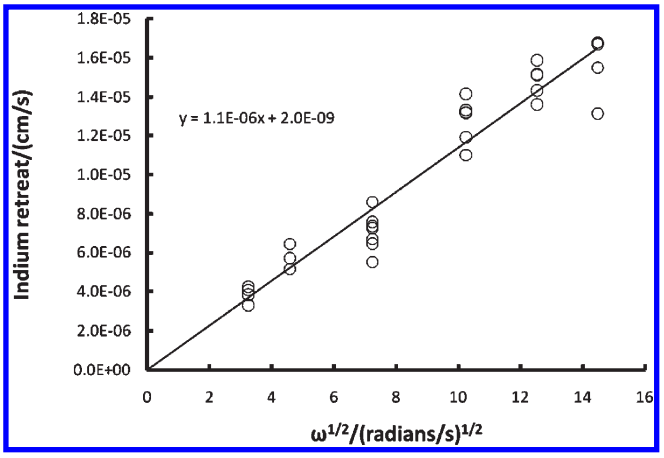

Figure 6. Rate of reaction vs the square root of the rotation rate for indium spheres on a rotator from 100 to 2000 rpm reacting with 0.1 M allyl bromide.

Table 5. Values of Apparent Rate Constant from Indium Spheres on a Rotating Shaft at 2000 rpm

allyl halide	k_{min}/(cm/s)	solvent[a]	solvent viscosity/cP
allyl iodide	7×10^{-3} cm/s	60/40/0.1	2.49
allyl bromide	9×10^{-3}	60/40/0.1	2.49
cinnamyl bromide	11×10^{-3}	90/10/0.1	1.71

[a] Solvent: ethanol %, water %, HCl/M.

rotation rate is linear. A plot of log(reaction rate) vs log(rotation rate) for allyl bromide (the same data as in Figure 6) has a slope of 0.49. A similar plot for allyl iodide has a slope of 0.52, and for cinnamyl bromide the slope is 0.55. The dependence on rotation rate demonstrates conclusively that the reaction is mass transport controlled under these conditions. The slope of the log−log plot being so close to 0.5 confirms that the Levich equation predicts well the effect of rotation rate for hemispheres that extend beyond the planar disk.

To determine the accuracy to which the Levich equation predicts the slope of the plot in Figure 6, the observed rate of retreat was converted to flux of allyl halide using eq 7, and the viscosity of 60/40/0.1 (Table 2) was converted to the kinematic viscosity in cm^2/s. Thus, the Levich equation predicts the slope of the plot of rate of retreat (dr/dt) vs $\omega^{1/2}$ (in Figure 6) to be 0.47×10^{-6} cm/s$^{1/2}$, while the observed value is approximately 2.3 times as large, 1.1×10^{-6} cm/s$^{1/2}$. The difference is probably attributable to the hemispheres extending above the surface of the rotating disk creating acceleration of the solution as it is pushed out of the way. To test this hypothesis, we revisited results from 18 experiments and compared the rate of retreat for the bead that extended furthest from the glue to that of the bead extending the least. On average, the more exposed beads protruded 0.27 mm further than the least exposed, and they reacted 1.43 times faster. Thus, this supports the idea of nonlaminar flow increasing the rate of reaction. Indeed, the characteristic asymmetric "shark fin" shape in Figure 5 is symptomatic of nonlaminar flow creating unequal mass transport over the surface of the hemisphere. A kinetically controlled reaction would be independent of mass transport and result in uniform retreat over the entire exposed surface of the sphere.

Table 6. Minimum Values of Heterogeneous Rate Constants

allyl halide	k_{min} MAG cell	k_{min} powder	k_{min} rotator
allyl iodide	5×10^{-4} cm/s	2×10^{-3} cm/s	6×10^{-3} cm/s
allyl bromide	4×10^{-4}	2×10^{-3}	9×10^{-3}
cinnamyl bromide	2×10^{-4}	2×10^{-3}	11×10^{-3}

The other two allyl halides also reacted at rates higher than those predicted by the Levich equation: allyl iodide reacted at 1.2 times the predicted rate and cinnamyl bromide at 1.9 times the predicted rate.

For ABr, a minimum value of k_s was calculated from k_{app} at 2000 rpm to be 9×10^{-3} cm/s (Table 5), higher than that determined by stirring in the "MAG" cells, powder, or glass−indium sandwiches.[26] For allyl iodide at 2000 rpm, $k_{min} = 6 \times 10^{-3}$ cm/s, and for cinnamyl bromide $k_{min} = 11 \times 10^{-3}$ cm/s.

CONCLUSION

Measurements of rates of reaction of allyl bromide, allyl iodide, and cinnamyl bromide demonstrate that their reaction with indium proceeds under mass transport control for the three different strategies of mass transport tested. Under mass transport control, the highest rates may be used to calculate the minimum value of the apparent heterogeneous rate constant, and these are summarized in Table 6. The values of k_{min} obtained by the rotator, 1×10^{-2} cm/s, are higher than those determined earlier[26] by an order of magnitude because the enhanced mass transport achievable with the rotator can detect transition to kinetic control with much larger minimum rate constants.

Each of the three strategies has advantages and disadvantages. Convection with traditional stir plates using MAG cells relies on relatively simple equipment. On the other hand, the mass transport is relatively slow and less reproducible than for the other strategies. Measurement of rates of reacting powder achieves faster mass transport, and experiments typically require less time (because the total distance of retreat is smaller) but require a compound microscope and are more challenging to do. Using a high precision, high speed rotator achieves the highest mass transport and the highest reproducibility of rates, but the rotator is relatively expensive.

Photomicroscopy using three new strategies is demonstrated to be a powerful tool for measuring rates of heterogeneous reactions in which the surface of a solid is retreating. The difference between mass transport and kinetic control is easily determined. For three allyl halides reacting with indium surfaces, mass transport controls the reaction rates, and the minimum values of k_s were determined to be 1×10^{-2} cm/s.

AUTHOR INFORMATION

Corresponding Author

*E-mail: bowyer@hws.edu. Phone: 315-781-3608. Fax: 315-781-3860.

ACKNOWLEDGMENT

This material is based upon work supported by the National Science Foundation under Grant No. CHE-1007510. We thank Richard Bolton, Peter Spacher, and Kathy Slentz of Hobart and William Smith Colleges for generous technical assistance.

REFERENCES

(1) Altman, E. L.; Schwarz, U. D. *Adv. Mater.* **2010**, *22*, 2854–2869.
(2) (a) Macpherson, J. V.; Simjee, N.; Unwin, P. R. *Electrochim. Acta* **2001**, *47*, 29–45.(b) Bard, A. J.; Faulkner, L. R. *Electrochemical Methods Fundamentals and Applications*; John Wiley and Sons: New York, 1980.
(3) Rogers, H. R.; Deutch, J.; Whitesides, G. M. *J. Am. Chem. Soc.* **1980**, *102*, 226–231.
(4) McCafferty, E. *Introduction to Corrosion Science*; Springer: New York, 2010.
(5) Koon, S. E.; Oyler, C. E.; Hill, J. H. M.; Bowyer, W. J. *J. Org. Chem.* **1993**, *58*, 3225–3226.
(6) Wittstock, G.; Burchardt, M.; Pust, S. E.; Shen, Y.; Zhao, C. *Angew. Chem., Int. Ed.* **2007**, *46*, 1548–1617.
(7) Engstrom, R. C.; Pharr, C. M. *Anal. Chem.* **1989**, *61*, 1099A–1104A.
(8) Bard, A. J.; Fan, F.-R. F.; Kwak, J.; Lev, O. *Anal. Chem.* **1989**, *61*, 132–138.
(9) Engstrom, R. C.; Weber, M.; Wunder, D. J.; Burgess, R.; Winquist, S. *Anal. Chem.* **1986**, *58*, 844–848.
(10) Greenwell, H. C.; Bindley, L. A.; Unwin, P. R.; Holliman, P. J.; Jones, W.; Coveney, P. V.; Barnes, S. L. *J. Cryst. Growth* **2006**, *294*, 53–59.
(11) Dobson, P. S.; Bindley, L. A.; Macpherson, J. V.; Unwin, P. R. *Langmuir* **2005**, *21*, 1255–1260.
(12) Engstrom, R. C.; Johnson, K. W.; DesJarlais, S. *Anal. Chem.* **1987**, *59*, 670–3.
(13) Bowyer, W. J.; Xie, J.; Engstrom, R. C. *Anal. Chem.* **1996**, *68*, 2005–9.
(14) Teerlinck, C. E.; Bowyer, W. J. *J. Org. Chem.* **1996**, *61*, 1059–1064.
(15) Biscoe, M. R.; Fry, A. J. *Tetrahedron Lett.* **2001**, *42*, 2759–2762.
(16) Beals, B. J.; Bello, Z. I.; Cuddihy, K. P.; Healy, E. M.; Koon-Church, S. E.; Owens, J. M.; Teerlinck, C. E.; Bowyer, W. J. *J. Phys. Chem. A* **2002**, *106*, 498–503.
(17) Simuste, H.; Panov, D.; Tuulmets, A.; Nguyen, B. T. *J. Organomet. Chem.* **2005**, *690*, 3061–3066.
(18) Jasien, P. G.; Abbondondola, J. A. *J. Mol. Struct. (Theochem)* **2004**, *671*, 111–118.
(19) Kim, S. H.; Lee, H. S.; Kim, K. H.; Kim, S. H.; Kim, J. N. *Tetrahedron* **2010**, *66*, 7065–7076.
(20) Roy, U. K.; Roy, S. *Chem. Rev.* **2010**, *110*, 2472–2535.
(21) Augé, J.; Lubin-Germain, N.; Uziel, J. *Synthesis* **2007**, *12*, 1739–1764.
(22) Kargbo, R. B.; Cook, G. R. *Curr. Org. Chem.* **2007**, *11*, 1287–1309.
(23) Paquette, L. A. *Synthesis* **2003**, *5*, 765–774.
(24) Koszinowski, K. *J. Am. Chem. Soc.* **2010**, *132*, 6032–6040.
(25) Bowyer, W. J.; Singaram, B.; Sessler, A. M. *Tetrahedron* **2011**, *67*, 7449−7460.
(26) Olson, I. A.; Sessler, A. M.; Connell, J. L.; Giordano, E.; Baez-Sosa, Y. Y.; Zavaleta, S. W.; Bowyer, W. J. *J. Phys. Chem. A* **2009**, *113*, 2801–2808.
(27) Araki, S.; Shimizu, T.; Johar, P. S.; Jin, S. J.; Butsugan, Y. *J. Org. Chem.* **1991**, *56*, 2538–2542.
(28) Andrieux, C. P.; Merz, A.; Saveant, J. M. *J. Am. Chem. Soc.* **1985**, *107*, 6097–6103.
(29) Rees, N. V.; Alden, J. A.; Dryfe, R. A. W.; Coles, B. A.; Compton, R. G. *J. Phys. Chem.* **1995**, *99*, 14813–8.
(30) Mbogoro, M. M.; Snowden, M. E.; Edwards, M. A.; Peruffo, M.; Unwin, P. R. *J. Phys. Chem. C* **2011**, *115*, 10147–54.
(31) Snowden, M. E.; King, P. H.; Covington, J. A.; Macpherson, J. V.; Unwin, P. R. *Anal. Chem.* **2010**, *82*, 3124–3131.
(32) Hutton, L. A.; Vidotti, M.; Iacobni, J. G.; Kelly, C.; Newton, M. E.; Unwin, P. R.; Macpherson, J. V. *Anal. Chem.* **2011**, *83*, 580408.
(33) Wightman, R. M.; Wipf, D. O. In *Electroanalytical Chemistry*; Bard, A. J., Ed.; Marcel Dekker: New York, 1989; Vol. 15, Chapter 3.
(34) Baur, J. E.; Wightman, R. M. *J. Electroanal. Chem.* **1991**, *305*, 73–81.
(35) Wehmeyer, K. R.; Wightman, R. M. *Anal. Chem.* **1985**, *57*, 1989–1993.
(36) McGeouch, C.-A.; Edwards, M. A.; Mbogoro, M. M.; Parkinson, C.; Unwin, P. R. *Anal. Chem.* **2010**, *82*, 9322–8.